

Progress in High-Precision Spectroscopy of Molecular
Ions in the Mid-Infrared

Charles Markus

Prospectus for Preliminary Examination

October 16th, 2015 1:00 PM

401 Roger Adams Laboratory

University of Illinois at Urbana-Champaign

1 Introduction

The structure and spectra of molecular ions are of significant interest to a number of scientific disciplines, ranging from molecular physics to astronomy. In order for *ab initio* techniques to accurately predict rovibrational transitions of complex molecules, the state of the art computational methods must be tested and refined using simple molecular systems. Many of the simplest systems are molecular ions, and their rovibrational spectra serve as valuable benchmarks for theorists. Also, in the cold and diffuse environment of the interstellar medium (ISM), ion - neutral reactions are the driving force behind chemical change. Their detection often depends on the existence of quality laboratory data. High-precision mid-infrared spectroscopy is a powerful tool in obtaining the experimental spectra required by both molecular theorists and astronomers.

Observing transitions of molecular ions is often a difficult challenge. Laboratory plasmas produce ions in low concentrations resulting in weak signals which can be obscured by the abundant neutral molecules. Velocity modulation spectroscopy enables the discrimination between signals from charged and neutral species [1]. This technique takes advantage of the fact that ions will oscillate in an AC driven discharge which results in a modulated signal, while neutrals remain relatively unaffected. This can be combined with the extremely sensitive technique noise immune cavity-enhanced optical heterodyne molecular spectroscopy (NICE-OHMS), which utilizes the path length enhancement from an optical cavity with the noise suppression of heterodyne spectroscopy [2]. These spectroscopic methods combined form the technique noise immune cavity-enhanced optical heterodyne velocity modulation spectroscopy (NICE-OHVMS) [3].

1.1 Instrument description

A detailed description of the instrument can be found in Hodges et al. [4], and a block diagram is shown in Figure 1. The light source is a high power continuous wave optical parametric oscillator (OPO). The OPO converts an input pump laser at 1064 nm into an idler beam, tunable from 3.2 - 3.9 μm , and a signal beam through parametric generation. An electro-optic modulator phase modulates the pump laser at the heterodyne frequency, which

imprints sidebands onto the idler beam. The idler is coupled into an external cavity where resonance is maintained using Pound-Drever-Hall (PDH) locking. Within the external cavity is a liquid-cooled positive column discharge cell known as “Black Widow”. Gas mixtures are flowed through the cell and a discharge is driven at ~ 50 kHz by a step-up transformer powered by an audio amplifier. Light transmitted through the cavity is focused onto a fast photodiode detector and the signal is first demodulated by two electronic mixers referenced 90 degrees out of phase with one another. The outputs are then sent to a pair of lock-in amplifiers referenced to twice the velocity modulation frequency. Both the in phase and quadrature components are recorded for each mixer, producing four total channels of detection.

The frequency of the idler is calculated by taking the difference of the pump and signal beam frequencies. Rough frequency determination is accomplished with an IR wavemeter, which is accurate to approximately 100 MHz. An optical frequency comb is used for highly accurate frequency calibration, which can determine the frequencies of the pump and signal beams within 10 kHz.

The line shape for a typical NICE-OHVMS scan can be seen in Figure 2. The combination of heterodyne and velocity modulation detection produce the odd line shape. With light propagating in both directions within the cavity, each component of the FM triplet can act to pump and probe. This produces several Lamb dips spaced at half integer multiples of the heterodyne frequency. The line centers can be determined to sub-MHz precision with a least squares fitting routine to the Lamb dips which is described by Crabtree et al. [5].

2 Completed Work

2.1 High-precision measurements of HeH^+

The molecular ion HeH^+ is the simplest heteronuclear molecule, making its potential energy surface (PES) of fundamental interest to *ab initio* theorists. Current calculations of its PES go beyond the Born-Oppenheimer approximation to include non-adiabatic, relativistic, and quantum electrodynamic (QED) corrections and are capable of predicting HeH^+ transitions within 0.01 cm^{-1} (300 MHz) [6]. Previously measured rovibrational transitions have uncer-

ainties of 0.002 - 0.005 cm^{-1} [7], and future refinements to *ab initio* predictions will require improved experimental data.

To improve upon the currently available data, we measured seven transitions spanning from $P(3)$ to $R(3)$ in the fundamental band of HeH^+ with sub-MHz precision ($3 \times 10^{-5} \text{cm}^{-1}$) [8]. With the newly measured transition frequencies, the rovibrational energy levels were calculated using combination differences. This information can be used by theorists to benchmark higher order corrections to the potential energy surface. The results and analysis of this work can be found in the attached paper by Perry et al. [8]. We also attempted an unsuccessful search for $v = 2 \leftarrow 1$ hot band transitions which were observed by Blom et al.[9]. Higher vibrational states allow for better understanding of the long range internuclear potential[10]. Unfortunately, it will likely require future improvements to the sensitivity of the instrument before this is possible.

2.2 Progress towards a high-precision H_3^+ survey

The molecular ion H_3^+ has been the focus of extensive study for its relevance to both the interstellar medium and molecular physics[11]. As the simplest polyatomic molecule, it serves as another important benchmark for *ab initio* theory. Adiabatic and relativistic corrections to the Born-Oppenheimer PES are capable of predicting transitions up to 6000 cm^{-1} with an accuracy of 0.1 cm^{-1} [12]. At lower rovibrational levels, non-adiabatic corrections using the core-mass approach have achieved an impressive accuracy 0.001 cm^{-1} (30 MHz) [13]. To evaluate future corrections and improvements to the PES, the energy level structure of H_3^+ can be constructed experimentally with high-precision rovibrational spectroscopy.

This will require measuring a large number of transitions in the fundamental band, while also requiring hot band and overtone transitions. Recently, we have measured 10 transitions with unprecedented precision in the R branch of the fundamental ν_2 band, which was a natural extension of the work previously accomplished using the NICE-OHVMS spectrometer by Hodges et al.[4]. The results from this work can be found in the attached paper by Perry et al.[14]. We also attempted to search for $2\nu_2^2 \leftarrow 1\nu_2^1$ hot band transitions, but again lacked the sensitivity to observe them. In order to continue this work, the coverage of the OPO will be expanded with additional modules and cavity mirrors. However, it is likely that the

sensitivity will also need to be improved in order to observe the hot band transitions.

2.3 High-precision spectroscopy of OH⁺

It has been a longstanding scientific objective of the NICE-OHVMS experiment to assist astronomical observations of rotational transitions by indirectly calculating them from rovibrational transitions. This led to the investigation of OH⁺, a molecule which is useful for constraining conditions in the interstellar medium. The relative abundance of OH⁺ to H₂O⁺ and H₃O⁺ depends on the cosmic ray ionization rate and the relative number densities of H₂ and free electrons [15]. In the past, water in the atmosphere prevented the detection of OH⁺ in interstellar environments. New high altitude and orbiting observatories have circumvented this problem and enabled detection of OH⁺ in the ISM.[16]. Because of the low temperatures in molecular clouds (30-100 K), a majority of OH⁺ observations have been of absorption from the ground rotational state with the exception of photon-dominated regions within our galaxy[17] and in the nearby galaxies Arp 220 and NGC 4418[18]. All observations of rotationally excited transitions have been with the instruments with moderate resolving power. Future detection will be limited to the German REceiver At Terahertz frequencies (GREAT) instrument aboard the Stratospheric Observatory For Infrared Astronomy (SOFIA), which has much higher resolving power and may require higher accuracy predictions than what is currently available.

The rotational structure of OH⁺ is due to its ³Σ⁻ ground electronic state, where the spin and rotational angular momentum couple as $\mathbf{J} = \mathbf{S} + \mathbf{N}$, where \mathbf{S} and \mathbf{N} are the spin and rotational angular momentum respectively. With a spin of $S = 1$, each level is split into a fine structure triplet of $J = N - 1, N, N + 1$. Each of these levels is further split into doublets by the proton spin of $I = 1/2$ into the total angular momentum $F = J \pm 1/2$. The only field-free rotational work has been of the $N = 1 \leftarrow 0$ [19] and the $N = 13 \leftarrow 12$ transitions [20]. Excited rotational transitions as high as $N = 3 \leftarrow 2$ have also been extrapolated from laser magnet resonance measurements(LMR)[21]. However, there have been cases where field-free transition frequencies had errors much larger than their claimed experimental uncertainties[22]. The remaining transitions have been determined indirectly from rovibrational data, where previous studies had an uncertainty of 90 MHz[23].

I sought to improve the THz predictions in order to facilitate observations of OH^+ in new sight lines. The ions were produced in a water-cooled discharge of H_2 and O_2 with He diluted in a He buffer gas. Although the signal to noise was much worse than previous ions we have studied, I was able to improve the line center frequencies for thirty transitions, from $P(5)$ to $R(5)$, with an average uncertainty of 2 MHz. The strongest transitions follow the selection rule $\Delta F = \Delta N = \Delta J$; although we were unable to resolve multiple components of the hyperfine structure, there were observed asymmetries in the Doppler profile in transitions with large hyperfine splitting. These 30 precise transition frequencies and all previous field free data available from the Cologne Database for Molecular Spectroscopy [24] were fit to a Dunham-type parameter set of an effective Hamiltonian for a $^3\Sigma^-$ linear molecule using the software SPFIT[25]. The new molecular constants were then used to predict a set of THz transitions. The uncertainties were improved by at least a factor of 2, which can be used to assist observations of rotationally excite OH^+ in the near future.

3 Proposed work

The two overarching scientific goals of the NICE-OHVMS instrument are to complete the high-precision survey of the H_3^+ molecule and to investigate the poorly understood IR spectrum of CH_5^+ . However, progress for both of these projects has been inhibited by the inability to detect and saturate the weaker transitions of these molecules. The baseline of NICE-OHVMS scans is not composed of random noise, but instead is a periodic signal which appears in all four channels with different strengths. This fringe is smothering weaker signals and will need to be overcome for our current objectives to be feasible. I propose to improve the NICE-OHVMS spectrometer by taking measures which will improve the signal to overcome the fringe and to mitigate the mechanisms which are causing it.

Observing the rovibrational spectrum of CH_5^+ will be a difficult task with the current configuration of the spectrometer. In the final section of this prospectus, I propose a method which will add millimeter-wave - infrared double-resonance functionality to the NICE-OHVMS spectrometer. This has the potential to give insight into the rotational and rovibrational structure of CH_5^+ that has never before been possible.

3.1 Reducing the fringe

Periodic background signals have long plagued sensitive spectroscopic measurements. In many cases it is due to unwanted etalons where only a small amounts of optical interference can quickly overcome weak absorption signals. The fringe we observe only appears during a discharge and has a period of ~ 30 MHz, which is independent of the scan rate. Given our detection scheme, there are likely two mechanisms responsible for the fringe. One contribution must be occurring at twice the velocity-modulation frequency to be detected by the lock-in amplifiers, and the second must be causing a frequency-dependent disturbance to the FM triplet.

A mechanism which would affect the signal at twice the velocity modulation frequency is the slight change in the index of refraction over a discharge cycle. For the “noise immunity” to be achieved in NICE-OHVMS, the heterodyne frequency must be an integer multiple the free spectral range (FSR) of the cavity, calculated by $\text{FSR} = c/2nl$ where c is the speed of light, n is the index of refraction, and l is the length of the cavity. The number density of all species within the discharge cell—i.e. ions, neutrals and free electrons—are modulated at twice the driving frequency which causes a time dependent refractive index within the external cavity[26]. This would cause the free spectral range to modulate at twice the velocity-modulation frequency causing a disruption to the FM triplet.

The frequency dependence of the signal strength could be explained by residual amplitude modulation (RAM) from the fiber coupled electro-optic modulator (FC-EOM) which has been observed in other NICE-OHMS experiments[27]. A misalignment of the optical fiber with the extraordinary axis of the lithium niobate crystal would cause the sidebands and carrier to undergo different phase shifts resulting in the FM triplet becoming unbalanced. This can be avoided with a proton-exchanged FC-EOM instead of using a titanium diffused EOM, which is what our system currently has. When a proton replaces Li^+ in the crystal lattice, it only increases the index of refraction along the extraordinary axis. This causes the EOM to only act as a waveguide for component aligned with the extraordinary axis which ignores the RAM-inducing misalignment.

3.2 Increasing the signal strength

NICE-OHVMS measures differences in phase or intensity between each component of the FM triplet, which are separated by the heterodyne-modulation frequency. To produce the strongest signal possible requires producing the largest differences between the carrier and the sidebands. For Doppler-broadened transitions this condition is met when the heterodyne frequency is approximately the full width at half maximum (FWHM) of the transition. The translational temperatures of our positive column result in line widths of 400-600 MHz while our heterodyne frequency is ~ 80 MHz which is far from ideal. It is feasible that the signal could be improved by a factor of 15 if a higher frequency were used, but this is not possible with the current detector which has a 3 dB bandwidth of ~ 150 MHz. However, near-infrared and optical detectors are much more sensitive can easily achieve a bandwidth of a few GHz. If the mid-IR light transmitted through the cavity were up-converted to an optical frequency using nonlinear optics, a faster detector could be used to detect the RF signal encoded in the light. One possible configuration would be to combine the 30 - 100 mW of idler power transmitted through the cavity with the output of a 10 W laser at 532 nm (Coherent Verdi v10) using sum frequency generation (SFG) with a periodically poled lithium niobate (PPLN) crystal. For this to be practical, the gains from the increased detector sensitivity and optimized heterodyne modulation must exceed the losses from conversion. In an ideal configuration, the SFG efficiency should be 1.4% which would produce 1 mW of power at 450 nm. Considering this, at 1 mW we would gain a factor of 325 in signal. Even with an efficiency 0.02% the signal would still be improved by a factor of 5. An added benefit will be resolving the sub-Doppler feature, which is composed of several Lamb-dips spaced at half integer multiples of the heterodyne frequency. Each Lamb dip is thought to have a width of approximately 60 MHz and is currently spaced at 40 MHz causing overlap. If we modulate as 320 or 400 MHz, we would be able to easily resolve the separate Lamb-dips. Fitting several narrow features instead of a wider blended feature would improve the simplicity of the fit and the precision of the line center determination.

Another opportunity to increase the signal would be to maximize the cavity enhancement. The signal enhancement in an external cavity is linear with respect to the cavity finesse, which

can be increased by reducing round trip losses. Currently the cavity is limited to a finesse of ~ 150 by the windows at the ends of discharge cell. It would be ideal if we were limited instead by the reflectivity of our cavity mirrors, which would be the case if they were mounted directly onto the cell using bellows. However, if the discharge were not properly contained it could damage the mirror surfaces and the piezoelectric transducer controlling the cavity length. A strong magnetic field could direct the electrons and ions into the walls of the cell, and NdFeB magnet should strong enough to prevent the discharge from reaching the mirrors. We could effectively move to much higher finesse with new high-reflectivity cavity mirrors with this configuration. A higher finesse will produce a steeper error signal for PDH locking, and might require faster corrections than the signal cavity PZT can provide (~ 1 kHz). Faster corrections on the order of a MHz would be possible with an acousto-optic modulator (AOM). Fiber coupled AOMs are available at frequencies for the pump laser and can be incorporated as long as diffraction losses do not lower the seed laser power below threshold for the fiber amplifier.

3.3 Infrared - millimeter-wave double-resonance spectroscopy

The molecular ion CH_5^+ has been a long standing challenge to theorists and spectroscopists. Calculations of its PES indicate that the five protons constantly rearrange through torsional and flipping motion between the 120 global potential energy minima [28]. The resulting large-amplitude motion complicates the rovibrational spectrum, which appears to have no discernible patterns[29]. However, the rotational structure could be relatively simple and allow for the effective geometry and potential surface of CH_5^+ to be determined[30].

Four-line combination differences are capable of revealing the underlying rotational structure from rovibrational transitions. As seen in Figure 3, if two sets of transitions have the same difference in energy it could indicate a separation of rotational energy levels. A large set of high-precision rovibrational frequencies could be used to calculate a large number of differences and separations in rotational energy levels will rise above the statistical noise. This has been accomplished with laser-induced reaction spectroscopy using a cold ion trap[31]. This approach could be performed using NICE-OHVMS, however in the spectrometer's current state it is only possible to measure a few of the strongest transitions. An alternative would

be to investigate the rotational transitions directly. The $J = 1 - 0$ transitions have been predicted to be within the millimeter-wave region of 220-235 GHz[32]. This could be accomplished by incorporating a millimeter-wave source to extend the NICE-OHVMS instrument into a double-resonance experiment.

Double-resonance spectroscopy observes the changes to a spectrum at a “probe” frequency in response to irradiation at a “pump” frequency. When the pump frequency is resonant with an allowed transition it will cause the population to oscillate between the two states. This oscillation occurs at the Rabi frequency, which depends on the intensity of light and the magnitude of the transition dipole moment. A second “probe” frequency, which is resonant with a different transition, will observe a change in signal if it is connected to one of the pumped states. An example would be a simple three level system seen in Figure 4, where levels 1 and 2 are separated by a millimeter-wave transition, and 2 and 3 are separated by a mid-infrared transition. A millimeter-wave source with sufficient intensity would bleach a component of the Doppler profile in the ground state, creating excess population in level 2 [33]. In order for the change in the Doppler profile to be observed without being “filled in” by collisions, the Rabi frequency must be comparable or greater than the collision rate[34]. At 0.5 Torr, collisional broadening of ions is on the order of 15 MHz. An extended interaction Klystron source can produce Watts of power at 220 GHz, and the CH_5^+ transition dipole moment for $J = 1 - 0$ is calculated to be between 1.5 - 1.6 D [32]. This would lead to a Rabi frequency of 20 MHz, which would be detectable.

First, the feasibility of the experiment will be tested on a molecule which has known rotational and rovibrational transitions at convenient frequencies. A possible candidate is the asymmetric top HOCS^+ which has its first rotational transition $J_{K_a, K_c} = 1_{0,1} \leftarrow 0_{0,0}$ at 11.453 GHz[35]. This is within a popular radar band where sources and amplifiers are readily available. The rovibrational transitions which could probe these states are the $J_{K_a, K_c} = 1_{0,1} \leftarrow 0_{0,0}$ and $J_{K_a, K_c} = 2_{0,2} \leftarrow 1_{0,1}$ in the fundamental band which are within the coverage of the OPO [36]. As long as it can be easily produced from a discharge of H_2 and OCS in a buffer gas, it would be an ideal molecule for testing the necessary conditions to acquire a double-resonance signal.

The amount of time spent searching for CH_5^+ transitions depends on the double-resonance

line width and the bandwidth of the lock-in amplifiers. For a given FWHM $W_{1/2}$ and lock-in time constant τ , the maximum scan rate can be calculated by the equation $r_s = 1.33W_{1/2}/8\tau$ [37]. The line widths should be broadened by collisions to approximately 15 MHz. If a time constant of 300 ms were used, a scan rate of 8 MHz/s would be attainable. This would cover the entire range of 15 GHz in 30 minutes of continuous scanning. The fourteen transitions which were observed in both the 4 K spectrum by Asvany et al. and the high temperature spectrum by White et al. would be ideal transitions to use as probes since they should be starting at the ground rotational state and be observable in our own positive column discharge.

4 Conclusion

By utilizing the sensitivity and precision afforded by NICE-OHVMS, a number of interesting molecular ions have been investigated which have interests in astronomy and fundamental physics. The work completed on HeH^+ and H_3^+ gives new target accuracies for *ab initio* theory. The investigation of OH^+ has given astronomers smaller search windows for important rotational transitions in new astronomical sight lines. The proposed improvements to the NICE-OHVMS spectrometer will allow for the completion of the H_3^+ survey and the ability to observe previously undetectable targets. The extension of the instrument into an infrared - millimeter-wave double-resonance spectrometer will allow for deeper understanding of the molecular ion CH_5^+ .

References

- [1] C. S. Gudeman, M. H. Begemann, J. Pfaff, and R. J. Saykally, "Velocity-modulated infrared laser spectroscopy of molecular ions: The ν_1 band of HNN^+ ," *J. Chem. Phys.*, vol. 78, no. 9, p. 5837, 1983.
- [2] J. Ye, L.-S. Ma, and J. L. Hall, "Ultrasensitive detections in atomic and molecular physics: demonstration in molecular overtone spectroscopy," *J. Opt. Soc. Am. B*, vol. 15, no. 1, p. 6, 1998.

- [3] B. M. Siller, M. W. Porambo, A. A. Mills, and B. J. McCall, “Noise immune cavity enhanced optical heterodyne velocity modulation spectroscopy,” *Optics express*, vol. 19, no. 24, pp. 24822–7, 2011.
- [4] J. N. Hodges, A. J. Perry, P. A. Jenkins, B. M. Siller, and B. J. McCall, “High-precision and high-accuracy rovibrational spectroscopy of molecular ions,” *J. Chem. Phys.*, vol. 139, p. 164201, Oct. 2013.
- [5] K. N. Crabtree, J. N. Hodges, B. M. Siller, A. J. Perry, J. E. Kelly, P. A. Jenkins, and B. J. McCall, “Sub-Doppler mid-infrared spectroscopy of molecular ions,” *Chem. Phys. Lett.*, vol. 551, pp. 1–6, Nov. 2012.
- [6] K. Pachucki and J. Komasa, “Rovibrational levels of helium hydride ion,” *J. Chem. Phys.*, vol. 137, no. 20, p. 204314, 2012.
- [7] P. Bernath and T. Amano, “Detection of the Infrared Fundamental Band of HeH^+ ,” *Phys. Rev. Lett.*, vol. 48, pp. 20–22, Jan. 1982.
- [8] A. J. Perry, J. N. Hodges, C. R. Markus, G. S. Kocheril, and B. J. McCall, “Communication: High precision sub-Doppler infrared spectroscopy of the HeH^+ ion,” *J. Chem. Phys.*, vol. 141, no. 10, p. 101101, 2014.
- [9] C. Blom, K. Möller, and R. Filgueira, “Gas discharge modulation using fast electronic switches: application to HeH^+ ,” 1987.
- [10] N. S. Dattani and M. Puchalski, “On the empirical dipole polarizability of He from spectroscopy of HeH^+ ,” *ArXiv*, pp. 1–5, 2014.
- [11] C. Lindsay and B. J. McCall, “Comprehensive Evaluation and Compilation of H_3^+ Spectroscopy,” *J. Mol. Spectrosc.*, vol. 210, pp. 60–83, Nov. 2001.
- [12] M. Pavanello, L. Adamowicz, A. Alijah, N. F. Zobov, I. I. Mizus, O. L. Polyansky, J. Tennyson, T. Szidarovszky, and A. G. Csaszar, “Calibration-quality adiabatic potential energy surfaces for H_3^+ and its isotopologues,” *J. Chem. Phys.*, vol. 136, no. 18, p. 184303, 2012.

- [13] L. G. Diniz, J. R. Mohallem, A. Alijah, M. Pavanello, L. Adamowicz, O. L. Polyansky, and J. Tennyson, “Vibrationally and rotationally nonadiabatic calculations on H_3^+ using coordinate-dependent vibrational and rotational masses,” *Phys. Rev. A*, vol. 88, no. 3, p. 032506, 2013.
- [14] A. J. Perry, J. N. Hodges, C. R. Markus, G. S. Kocheril, and B. J. McCall, “High-precision R-branch transition frequencies in the ν_2 fundamental band of H_3^+ ,” *J. Mol. Spectrosc.*, pp. 10–12, 2015.
- [15] N. Indriolo, D. A. Neufeld, M. Gerin, T. R. Geballe, J. H. Black, K. M. Menten, and J. R. Goicoechea, “CHEMICAL ANALYSIS OF A DIFFUSE CLOUD ALONG A LINE OF SIGHT TOWARD W51: MOLECULAR FRACTION AND COSMIC-RAY IONIZATION RATE,” 2012.
- [16] F. Wyrowski, K. M. Menten, R. Güsten, and A. Belloche, “First interstellar detection of OH^+ ,” *Astron. Astrophys.*, vol. 518, p. A26, July 2010.
- [17] F. V. D. Tak, Z. Nagy, and V. Ossenkopf, “Spatially extended OH^+ emission from the Orion Bar and Ridge,” *Astron. Astrophys.*, vol. 95, pp. 1–10, 2013.
- [18] E. González-Alfonso, J. Fischer, S. Bruderer, H. S. P. Müller, J. Graciá-Carpio, E. Sturm, D. Lutz, A. Poglitsch, H. Feuchtgruber, S. Veilleux, A. Contursi, A. Sternberg, S. Hailey-Dunsheath, A. Verma, N. Christopher, R. Davies, R. Genzel, and L. Tacconi, “Excited OH^+ , H_2O^+ , and H_3O^+ in NGC 4418 and Arp 220,” *Astron. Astrophys.*, vol. 550, p. A25, 2013.
- [19] J. P. Beokooy, P. Verhoeve, W. L. Meerts, and A. Dymanus, “Submillimeter spectroscopy on OH^+ : The rotational transition at 1 THz,” *J. Chem. Phys.*, vol. 82, no. 8, p. 3868, 1985.
- [20] D.-J. Liu, W.-C. Ho, and T. Oka, “Rotational spectroscopy of molecular ions using diode lasers,” *J. Chem. Phys.*, vol. 87, no. 5, p. 2442, 1987.

- [21] M. H. W. Gruebele, R. P. Müller, and R. J. Saykally, “Measurement of the rotational spectra of OH⁺ and OD⁺ by laser magnetic resonance,” *J. Chem. Phys.*, vol. 84, no. 5, p. 2489, 1986.
- [22] V. Ossenkopf, H. S. P. Müller, D. C. Lis, P. Schilke, T. A. Bell, S. Bruderer, E. Bergin, C. Ceccarelli, C. Comito, J. Stutzki, A. Bacman, A. Baudry, A. O. Benz, M. Benedettini, O. Berne, G. Blake, A. Boogert, S. Bottinelli, F. Boulanger, S. Cabrit, P. Caselli, E. Caux, J. Cernicharo, C. Codella, A. Coutens, N. Crimier, N. R. Crockett, F. Daniel, K. Demyk, P. Dieleman, C. Dominik, M. L. Dubernet, M. Emprechtinger, P. Encrenaz, E. Falgarone, K. France, A. Fuente, M. Gerin, T. F. Giesen, A. M. di Giorgio, J. R. Goicoechea, P. F. Goldsmith, R. Güsten, A. Harris, F. Helmich, E. Herbst, P. Hily-Blant, K. Jacobs, T. Jacq, C. Joblin, D. Johnstone, C. Kahane, M. Kama, T. Klein, A. Klotz, C. Kramer, W. Langer, B. Lefloch, C. Leinz, A. Lorenzani, S. D. Lord, S. Maret, P. G. Martin, J. Martin-Pintado, C. McCoey, M. Melchior, G. J. Melnick, K. M. Menten, B. Mookerjee, P. Morris, J. A. Murphy, D. a. Neufeld, B. Nisini, S. Pacheco, L. Pagani, B. Parise, J. C. Pearson, M. Pérault, T. G. Phillips, R. Plume, S.-L. Quin, R. Rizzo, M. Röllig, M. Salez, P. Saraceno, S. Schlemmer, R. Simon, K. Schuster, F. F. S. van der Tak, A. G. G. M. Tielens, D. Teyssier, N. Trappe, C. Vastel, S. Viti, V. Wakelam, A. Walters, S. Wang, N. Whyborn, M. van der Wiel, H. W. Yorke, S. Yu, and J. Zmuidzinas, “Detection of interstellar oxidaniumyl: Abundant H₂O⁺ towards the star-forming regions DR21, Sgr B2, and NGC6334,” *Astron. Astrophys.*, vol. 518, p. L111, July 2010.
- [23] B. D. Rehfuss, M.-F. Jagod, L.-W. Xu, and T. Oka, “Infrared spectroscopy of highly excited vibrational levels of the hydroxyl ion, OH⁺,” 1992.
- [24] H. S. P. Müller, F. Schlöder, J. Stutzki, and G. Winnewisser, “The Cologne Database for Molecular Spectroscopy, CDMS: A useful tool for astronomers and spectroscopists,” *J. Mol. Struct.*, vol. 742, no. 1-3, pp. 215–227, 2005.
- [25] H. M. Pickett, “The fitting and prediction of vibration-rotation spectra with spin interactions,” *J. Mol. Spectrosc.*, vol. 148, no. 2, pp. 371–377, 1991.

- [26] U. Ascoli-Bartoli, A. De Angelis, and S. Martellucci, “Wavelength dependence of the refractive index of a plasma in the optical region,” *Nuovo Cim.*, vol. 18, pp. 1116–1137, Dec. 1960.
- [27] A. Foltynowicz, I. Silander, and O. Axner, “Reduction of background signals in fiber-based NICE-OHMS,” *J. Opt. Soc. Am. B*, vol. 28, p. 2797, Oct. 2011.
- [28] X. Huang, A. B. McCoy, J. M. Bowman, L. M. Johnson, C. Savage, F. Dong, and D. J. Nesbitt, “Quantum deconstruction of the infrared spectrum of CH_5^+ ,” *Science*, vol. 311, pp. 60–3, Jan. 2006.
- [29] E. T. White, J. Tang, and T. Oka, “ CH_5^+ : The Infrared Spectrum Observed,” *Science*, vol. 284, pp. 135–137, Apr. 1999.
- [30] P. R. Bunker, “Energy Levels and Spectrum of CH_5^+ ,” vol. 304, no. 176, pp. 297–304, 1996.
- [31] O. Asvany, K. M. T. Yamada, S. Brunken, A. Potapov, and S. Schlemmer, “Experimental ground-state combination differences of CH_5^+ ,” *Science*, vol. 347, pp. 1346–1349, Mar. 2015.
- [32] P. R. Bunker, B. Ostojić, and S. Yurchenko, “A theoretical study of the millimeter-wave spectrum of CH_5^+ ,” *J. Mol. Struct.*, vol. 695-696, pp. 253–261, 2004.
- [33] T. Oka, “Intracavity Infrared-Microwave Double-resonance Spectroscopy,” *Philos. Trans. A. Math. Phys. Eng. Sci.*, vol. 307, pp. 591–601, 1982.
- [34] E. Arimondo, P. Glorieux, and T. Oka, “Radio-frequency spectroscopy inside a laser cavity; ”pure” nuclear quadrupole resonance of gaseous CH_3I ,” *Phys. Rev. A*, vol. 17, pp. 1375–1393, Apr. 1978.
- [35] Y. Ohshima and Y. Endo, “Rotational spectroscopy of jet-cooled molecular ions and ion complexes,” *Chem. Phys. Lett.*, vol. 256, pp. 635–640, July 1996.
- [36] T. Nakanaga and T. Amano, “High-resolution infrared identification of HOCS^+ with difference frequency laser spectroscopy,” *Mol. Phys.*, vol. 61, pp. 313–323, June 1987.

[37] W. E. Blass and G. W. Halsey, "Introduction," in *Deconvolution Absorption Spectra*, p. 6, Elsevier, 1981.

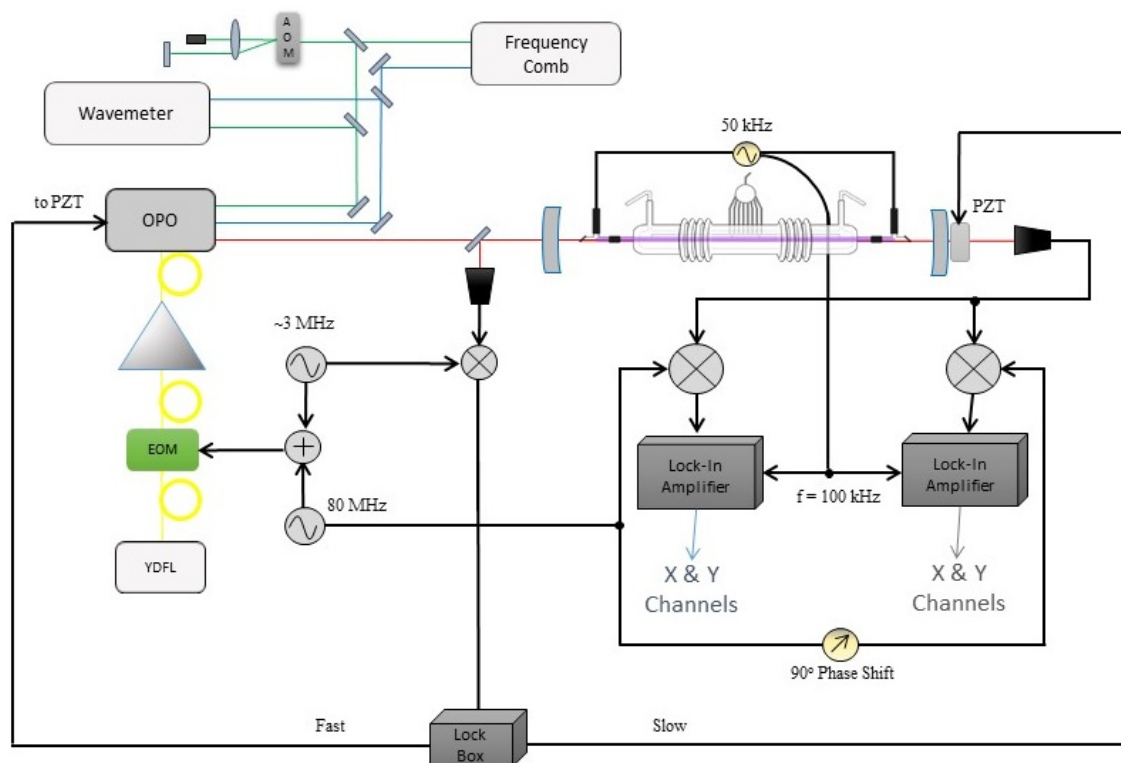


Figure 1: A block diagram of the NICE-OHVMS spectrometer, the idler is shown in red, pump beam in blue, signal in green. (YDFL: ytterbium doped fiber laser, EOM: electro-optic modulator, OPO: optical parametric oscillator, PZT: piezo transducer)

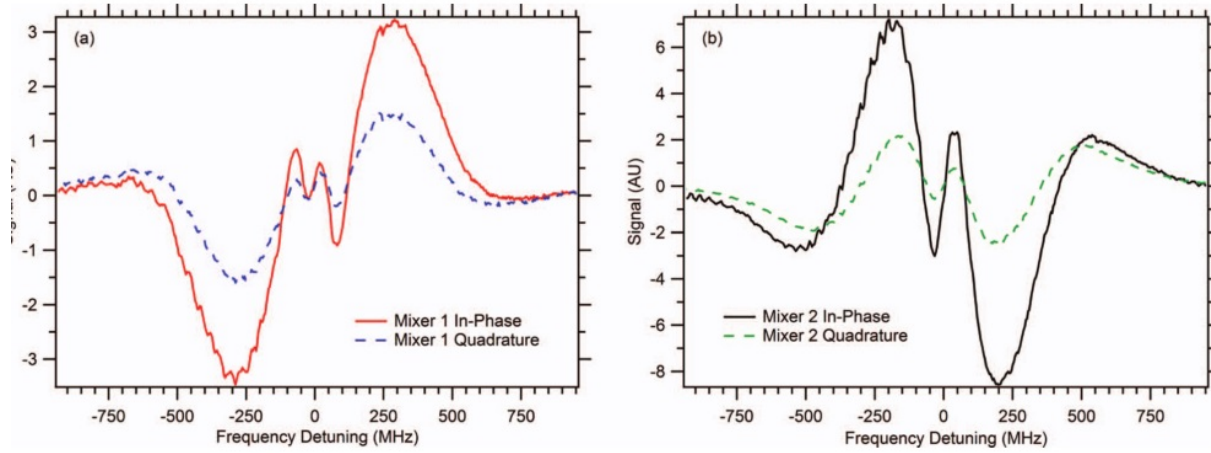


Figure 2: A typical NICE-OHVMS scan showing the P(1) transition in the fundamental band of HeH^+ , the feature at the center is the Lamb dip while the larger shape is the Doppler profile. The in-phase output of the lock-in amplifiers are shown in solid red and black, while the quadrature trace is represented by the blue and green dashed lines. Panel (a) represents the output from mixer1 and panel (b) represents mixer 2 [8].

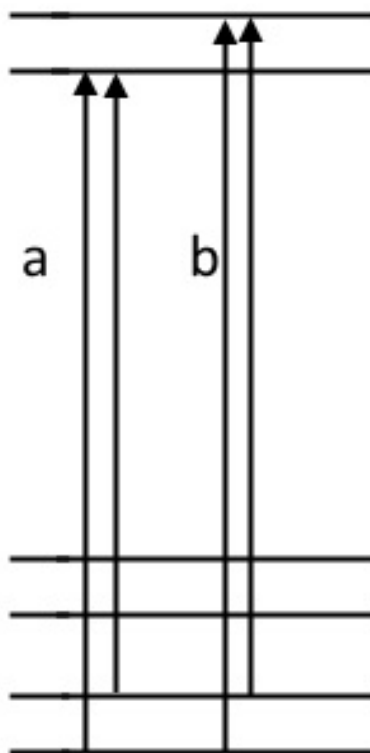


Figure 3: An example of a four line combination difference. Both pairs a and b originate from the same two states, and therefore the difference in frequency is the same for both pairs.

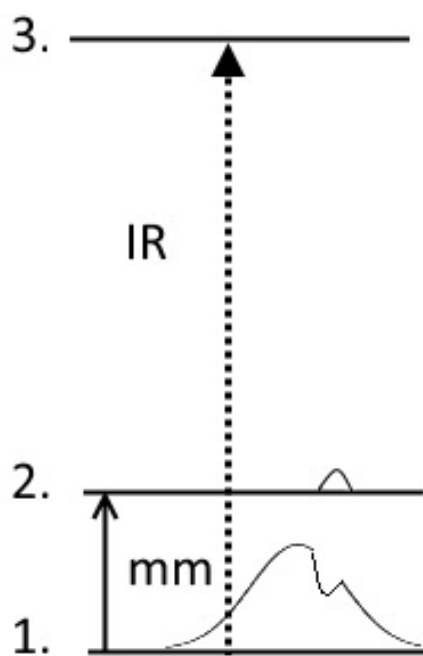


Figure 4: A representation of a three level double-resonance experiment where the millimeter-wave radiation pumps the molecules from level 1 to 2. The infrared radiation can then probe the change in population by observing a change in signal.

Communication: High precision sub-Doppler infrared spectroscopy of the HeH⁺ ion

Adam J. Perry, James N. Hodges, Charles R. Markus, G. Stephen Kocheril, and Benjamin J. McCall

Citation: *The Journal of Chemical Physics* **141**, 101101 (2014); doi: 10.1063/1.4895505

View online: <http://dx.doi.org/10.1063/1.4895505>

View Table of Contents: <http://scitation.aip.org/content/aip/journal/jcp/141/10?ver=pdfcov>

Published by the [AIP Publishing](#)

Articles you may be interested in

Communication: He-tagged vibrational spectra of the SarGlyH⁺ and H+(H₂O)_{2,3} ions: Quantifying tag effects in cryogenic ion vibrational predissociation (CIVP) spectroscopy

J. Chem. Phys. **140**, 221101 (2014); 10.1063/1.4880475

Properties of the B⁺-H₂ and B⁺-D₂ complexes: A theoretical and spectroscopic study

J. Chem. Phys. **137**, 124312 (2012); 10.1063/1.4754131

Rotationally resolved infrared spectrum of the Na⁺-D₂ complex: An experimental and theoretical study

J. Chem. Phys. **134**, 214302 (2011); 10.1063/1.3596720

A three-dimensional ab initio potential energy surface and predicted infrared spectra for the He – N₂ O complex

J. Chem. Phys. **124**, 144317 (2006); 10.1063/1.2189227

Infrared laser absorption spectroscopy of rotational and vibration rotational transitions of HeH⁺ up to the dissociation threshold

J. Chem. Phys. **107**, 337 (1997); 10.1063/1.474394



COMSOL
CONFERENCE
2014 BOSTON

The Multiphysics
Simulation
Event of the Year

LEARN MORE >>

COMSOL

Communication: High precision sub-Doppler infrared spectroscopy of the HeH⁺ ion

Adam J. Perry,¹ James N. Hodges,¹ Charles R. Markus,¹ G. Stephen Kocheril,¹ and Benjamin J. McCall^{1,2,a)}

¹Department of Chemistry, University of Illinois, Urbana, Illinois 61801, USA

²Departments of Astronomy and Physics, University of Illinois, Urbana, Illinois 61801, USA

(Received 30 July 2014; accepted 28 August 2014; published online 9 September 2014)

The hydrohelium cation, HeH⁺, serves as an important benchmark for *ab initio* calculations that take into account non-adiabatic, relativistic, and quantum electrodynamic effects. Such calculations are capable of predicting molecular transitions to an accuracy of ~ 300 MHz or less. However, in order to continue to push the boundaries on these calculations, new measurements of these transitions are required. Here we measure seven rovibrational transitions in the fundamental vibrational band to a precision of ~ 1 MHz using the technique of Noise Immune Cavity Enhanced Optical Heterodyne Velocity Modulation Spectroscopy. These newly measured transitions are included in a fit to the rotation-vibration term values to derive refined spectroscopic constants in the $v = 0$ and $v = 1$ vibrational states, as well as to calculate rotation-vibration energy levels with high precision.

© 2014 AIP Publishing LLC. [<http://dx.doi.org/10.1063/1.4895505>]

I. INTRODUCTION

Composed of the two most abundant elements in the universe, the HeH⁺ cation is predicted to be among the first molecules ever formed,^{1,2} which makes this species of vital significance to chemical models of the early universe. Astronomical observations targeted at HeH⁺ have yet to yield an unequivocal detection of this molecule. The difficulty in detecting this species is attributed to the many chemical processes that compete with the formation of HeH⁺, ultimately resulting in a low abundance of this molecule. However, this molecule is easily formed in laboratory plasmas, which has spurred much experimental work on this fundamental species.

First discovered in 1925,³ the HeH⁺ ion has been the subject of many spectroscopic studies. In 1979, the first rovibrational spectrum of this molecule was acquired by Tolliver and co-workers, who observed the P(12) and P(13) lines in the fundamental vibrational band as well as the P(9)-P(11) transitions in the $v = 2 \leftarrow 1$ hot band with an accuracy of ~ 0.002 cm⁻¹.⁴ In 1982, Bernath and Amano reported the first observation of the low J transitions in the fundamental band, covering the P(4)-R(4) rovibrational transitions.⁵ After this work various studies of hot bands were published, including transitions from bound to quasibound states as well as quasibound to quasibound transitions.⁶⁻⁸ In 1989, Crofton and co-workers measured a few new transitions in the fundamental band along with several lines in the $v = 2 \leftarrow 1$ hot band as well as in the fundamental bands of the ³HeH⁺, ⁴HeD⁺, and ³HeD⁺ isotopologues.⁹ Pure rotational studies were first carried out by Liu *et al.* where the $J = 7 \leftarrow 6$ transition was measured,¹⁰ followed by the measurement of $J = 1 \leftarrow 0$ and $J = 2 \leftarrow 1$ by Matsushima *et al.*¹¹ as well as some low J

rotational transitions of the ³HeH⁺, ⁴HeD⁺, and ³HeD⁺ isotopologues. Higher J rotational transitions were measured by Liu and Davies^{8,12} with J as high as 25.

From a theoretical standpoint the HeH⁺ ion is a relatively simple species that is isoelectronic to H₂. This makes HeH⁺ an important benchmark molecule for high-level *ab initio* calculations that take into account not only non-adiabatic corrections to the Born Oppenheimer approximation, but also relativistic and quantum electrodynamic (QED) effects. Recent *ab initio* calculations by Pachucki and Kosama,¹³ which have treated the non-adiabatic corrections using Non-Adiabatic Perturbation Theory as well as the relativistic (α^2) and leading QED (α^3) corrections to the Born-Oppenheimer approximation, have been able to reproduce many experimentally measured rovibrational transitions with an accuracy on the order of 0.01 cm⁻¹ (~ 300 MHz). This sort of accuracy is only currently achievable for a select few molecular systems, namely, H₂, H₂⁺, H₃⁺, and HeH⁺.¹³⁻¹⁷ In order to predict transition frequencies with accuracies on the level of 0.001 cm⁻¹ or better for more complicated systems, it is imperative that the theoretical treatment of the aforementioned benchmark systems be well developed. Since theory must be informed by experiment to push the boundaries of these calculations, experimentalists need to provide highly accurate and precise measurements of molecular transitions for these species.

The HeH⁺ molecule has also proven to be a useful benchmark system for theoretical treatments that go beyond the Born-Oppenheimer approximation.¹⁸ These methods rely on using a set of correlated Gaussian functions that are functions of the separations between the nuclei and electrons, thus eliminating the traditional separation of the nuclear and electronic wavefunctions of the Born-Oppenheimer approximation. Within this framework the authors also developed algorithms for calculating the complete relativistic correction for this molecule.^{19,20} To date, these sorts of calculations have

^{a)}Electronic mail: bjmccall@illinois.edu

only been performed on states with no angular momentum (i.e., “rotationless” states).

Another approach has been to develop a global empirical potential that is based on the available spectroscopic data.²¹ This work used all available spectroscopic data from all isotopomers in a fit to a modified Lennard-Jones potential that is able to provide the correct behavior at large internuclear separations near the dissociation limit. This approach also allows for experimental determination of the Born-Oppenheimer breakdown functions which showed reasonable agreement with a fitted theoretical potential based on the calculations of Bishop and Cheung.²²

II. EXPERIMENTAL

The instrument used in this work has been described in detail in Ref. 23 and therefore will be described here only briefly. For this work, we used a technique that has been previously developed in our lab called Noise Immune Cavity Enhanced Optical Heterodyne Velocity Modulation Spectroscopy (NICE-OHVMS)^{23–25} which combines the high sensitivity of Noise Immune Cavity Enhanced Optical Heterodyne Molecular Spectroscopy (NICE-OHMS)²⁶ with the ion/neutral discrimination of velocity modulation spectroscopy.²⁷

The spectrometer is based on a commercially available continuous wave optical parametric oscillator (Aculight Argos 2400 SF) that is tunable across the 3.2–3.9 μm range. The pump laser (Koheras Adjustik Y-10) is phase modulated at a frequency of ~ 80 MHz to produce a pair of RF sidebands that are imprinted onto the idler wave. The idler wave is then coupled into an external optical cavity (finesse of ~ 150) which surrounds a liquid nitrogen cooled positive column discharge cell, in which ions of interest are produced from precursor gasses (a 2 Torr mixture of H_2 and He in a 1:100 ratio) and where their absorption profiles are velocity modulated. Light transmitted through the cavity is detected by a fast photodiode detector (Boston Electronics Vigo PVM-10.6-1 \times 1), from which the signal is demodulated at the same frequency used

to generate the 80 MHz sidebands, using a pair of frequency mixers that are 90° out of phase with one another. Further demodulation of the mixer outputs at twice the velocity modulation frequency (~ 80 kHz) is accomplished by a pair of lock-in amplifiers, which acts to recover the velocity modulation information.

Frequency calibration of our spectra was accomplished using an optical frequency comb (Menlo Systems FC-1500 with 100 MHz repetition rate) to measure the difference in frequency of the pump and signal beams at each point. Initial measurements of the frequencies of both beams (ten measurements for each) are performed using a near-infrared wavemeter (Burleigh WA-1500) to determine the mode number of the nearest comb tooth. The accuracy of the wavemeter was enhanced by measuring nearby reference lines of CH_4 .²⁸ These reference line frequencies are all determined to within ~ 5 MHz and any systematic errors introduced by the wavemeter can be corrected to ensure that the proper comb mode numbers are determined.

III. RESULTS

Figure 1 shows a typical NICE-OHVMS spectrum of the P(1) transition of HeH^+ at 85258146.86(35) MHz. The line-shapes have an odd symmetry resulting from the heterodyne detection and velocity modulation schemes. The narrow features near the center of the lines are blends of several individual Lamb dips that are spaced by half-integer multiples of the heterodyne frequency about the center of the transition. To extract the transition line centers, we fit the data from all four of the detection channels simultaneously (Figure 2) with some shared parameters between the data channels such as the line center, full-width of the blended feature, and the heterodyne detection angle. Further information regarding the fitting routines has been given by Hodges *et al.*²³

Table I shows that our measurements exhibit good agreement with the values measured by Bernath and Amano as all measured transitions lie within or only slightly outside their 30–60 MHz claimed uncertainties. However, in this work we

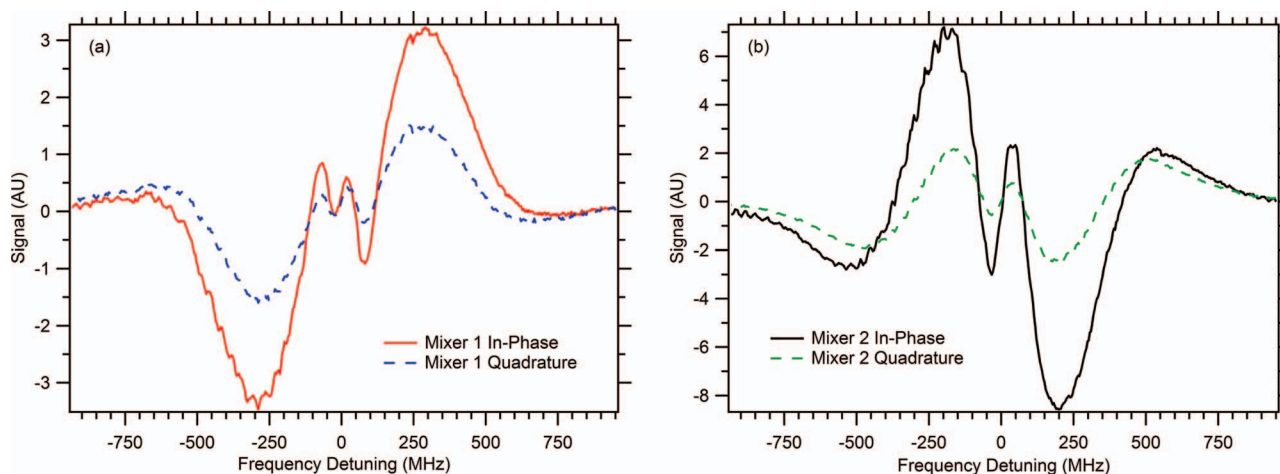


FIG. 1. Typical NICE-OHVMS scan of the P(1) fundamental band transition of HeH^+ showing the central Lamb dip feature sitting on top of the Doppler profile of the line. Signals from each of the four detection channels are shown with the in-phase (red solid trace) and quadrature (blue dashed trace) channels from mixer 1 plotted in panel (a) and the in-phase (black solid trace) and quadrature (green dashed trace) channels of mixer 2 in panel (b).

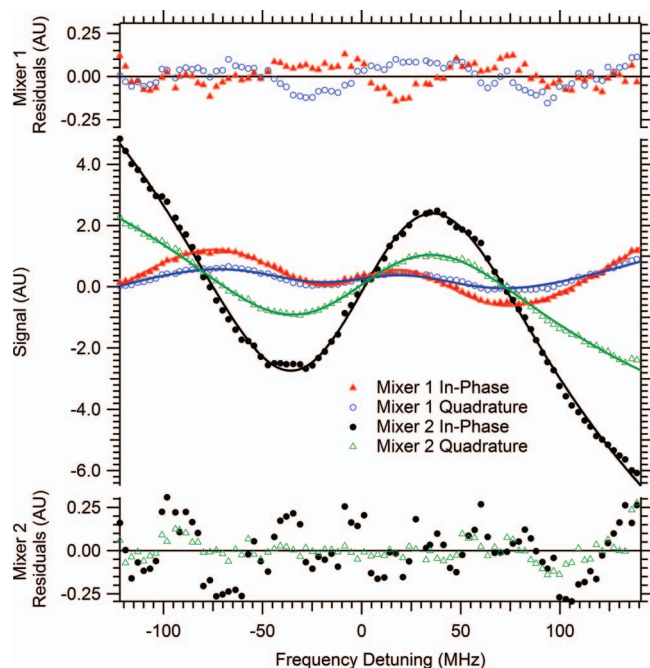


FIG. 2. Frequency comb calibrated scan of the central sub-Doppler Lamb dip feature in the P(1) rovibrational transition of HeH^+ , along with a simultaneous fit of all four data acquisition channels. Colored markers represent the experimental data, while the colored solid traces show the fit of the data to the equation outlined in Hodges *et al.*²³ Fit residuals from each detection channel are plotted on the upper (channels from mixer 1) and lower (channels from mixer 2) axes. For clarity, only every third data point is shown.

have improved the precision on these measurements by two orders of magnitude. For all of the measurements we were able to obtain precisions on the order of 1 MHz for the line centers due to both our ability to saturate the transitions which allows us to fit the relatively narrow sub-Doppler features, and the frequency calibration provided by the optical frequency comb which allows us to go far beyond the typical tens of MHz measurement uncertainty provided by mid-infrared wavemeters and Doppler-broadened reference gas lines.

These new measurements together with all available data for the fundamental band^{4,5,7,9} as well as pure rotational data^{8,10,11} were included in a fit to a power-series expansion of the vibration-rotation term values for a $^1\Sigma$ linear molecule as shown in Eq. (1) [The measurements of P(9)-P(11) by Purder *et al.* were not included in the fit as no uncertainties were

TABLE I. All measured rovibrational transitions in the fundamental vibrational band of HeH^+ and a comparison to those values measured by Bernath and Amano.⁵ All units are in MHz.

Transition	Freq.	St. Dev.	Prev. value ⁵	Diff.
P(3)	80795499.88	0.99	80795566.39	-66.51
P(2)	83096617.69	1.34	83096650.39	-32.69
P(1)	85258146.86	0.35	85258082.06	64.80
R(0)	89115533.66	1.38	89115502.62	31.04
R(1)	90788380.66	0.40	90788398.50	-17.84
R(2)	92275879.63	0.77	92275875.74	3.89
R(3)	93567523.38	0.92	93567519.55	3.82

TABLE II. Rovibrational parameters from a fit of experimentally measured rotation and rovibration transitions to Eq. (1). All units are in MHz.

Parameter	This work	Liu and Davies ⁸
ν_0	87268330.62(54)	87268319(33)
B_0	1006063.39(15)	1006063.3(45)
D_0	486.1762(187)	486.512(96)
H_0	0.1807358(2628)	0.18428(84)
$L_0 \times 10^4$	-1.17975(1418)	-1.331(36)
$M_0 \times 10^7$	0.73228(3114)	1.022(69)
$N_0 \times 10^{10}$	-0.49376(2392)	-0.702(48)
B_1	924550.54(17)	924554.8(45)
D_1	475.1636(138)	475.606(99)
H_1	0.1660888(3241)	0.17049(84)
$L_1 \times 10^4$	-1.31950(2056)	-1.499(33)
$M_1 \times 10^7$	1.05510(4957)	1.385(60)
$N_1 \times 10^{10}$	-1.12488(4121)	-1.352(42)

reported],²⁹

$$F_v = G_v + B_v J(J+1) - D_v [J(J+1)]^2 + H_v [J(J+1)]^3 + L_v [J(J+1)]^4 + M_v [J(J+1)]^5 + N_v [J(J+1)]^6. \quad (1)$$

The fit was performed using PGOPHER,³⁰ floating all parameters in both the ground and first excited vibrational states. In addition to our high-precision rovibrational measurements and the remaining fundamental band data, the fit includes the two pure rotational transitions ($J = 1 \leftarrow 0$ and $J = 2 \leftarrow 1$) measured by Matsushima *et al.* with very high precision (~ 200 kHz), as well as the pure rotational transitions of Liu and Davies, which includes 11 transitions in both the $v = 0$ and $v = 1$ vibrational states covering a range of J'' from 10 to 20. Parameters from the fit are given in Table II along with a comparison to those values obtained by Liu and Davies.⁸ Full details of the fit can be found in the supplementary material.³¹ Inclusion of these high precision measurements allows for a more precise determination (by roughly an order of magnitude) of the band origin as well as the B rotational constants and the lower order centrifugal distortion terms up to H.

It is interesting to note that for all the centrifugal distortion terms there are significant differences between our values and those of Liu and Davies. However, the results of the fit showed that the weighted residuals were randomly distributed across the entire range of J'' , which suggests that the differences in the fit parameters may be due to a high degree of correlation among the higher order parameters. Indeed, when the correlation matrix is examined it is clear that this is the case as the H, L, M, and N parameters all show correlations of ≥ 0.9 with each other.

Another comparison can be made to the fit produced by Matsushima *et al.*¹¹ In their fit they only included their $J = 1 \leftarrow 0$ and $J = 2 \leftarrow 1$ transitions along with the available rovibrational data in the fundamental band, while only including terms up to L (the values of L were fixed to the *ab initio* predictions of Bishop and Cheung²²). By doing so they were able to obtain very precise values for the B, D, and H values, which are nearly an order of magnitude more precise

TABLE III. Experimentally determined rotation-vibration energy levels $E(v,J)$ for ${}^4\text{HeH}^+$. All units are in MHz.

J	$E(0,J)$	$E(1,J)$
0	0	87268330.76(41)
1	2010183.86(20)	89115533.7(14)
2	6018916.87(28)	92798564.52(44)
3	12003064.7(11)	98294796.51(83)
4	19928164(60)	105570588.0(14)
5	29749118(30)	114581537(85)
6	41409933(172)	125273098(153)
7	54845432(194)	137580625(228)
8		151431127(245)

than the values reported in Table II. It may be the case, however, that the quality of their fit was somewhat fortuitous, due to the weighting of the highly precise values for the rotational transitions and their influence on the values of the lower order rotational parameters. We conjecture that since these lower order parameters were tightly constrained by only two transitions, their fit may have yielded well-determined parameters because there was so much more relative uncertainty in the rovibrational transition frequencies. The inclusion of our data, which also probe the $J = 0, 1,$ and 2 levels in the ground vibrational state and carry a similar weighting in the fit as Matsushima's rotational transitions, may explain the apparent increase in the uncertainty of our parameters.

To further assess the accuracy of our measurements we performed a test by adding Gaussian noise of varying amounts (as determined by the standard deviation of this added noise) to our transition frequencies and running the fit described above using these modified frequencies. For noise with a standard deviation of 2 MHz we begin to see a noticeable degradation in the quality of the fit in terms of the residuals of our seven measured transitions. With this amount of "noise" we find that the RMS of the residuals for these seven transitions increases by roughly a factor of two. Though this test may not be 100% conclusive due to the random nature of adding in this noise, it does give us confidence that our claimed uncertainties are appropriate in size.

Using these new data along with previous infrared and pure rotational work, a set of experimentally determined rovibrational energy levels can be derived using a combination difference analysis. Evaluating the energy levels in this way is advantageous because they are not based on any model Hamiltonian. The energy levels covering $J = 0-7$ in the vibrational ground state and $J = 0-8$ in the $v = 1$ vibrational excited state can be computed based on the available spectroscopic data. Table III summarizes the results.

The high precision (no larger than 1.4 MHz) of the $J = 3$ level in the ground vibrational state and the first five rotational levels in the $v = 1$ vibrational state, will allow these energy levels to serve as excellent benchmark values for new *ab initio* calculations on this molecule.

IV. CONCLUSION

We have performed sub-Doppler mid-infrared spectroscopy on the HeH^+ cation. By using the technique of

NICE-OHVMs in conjunction with frequency calibration provided by an optical frequency comb, we have re-measured seven fundamental band transitions of this molecule with a precision on the order of 1 MHz, and were able to achieve sub-MHz precision on most of the measured transitions. Using these new transitions with their improved uncertainties we have improved the values of the band origin as well as the B rotational constants and the lower order centrifugal distortion terms in a fit that includes all available spectroscopic data for the $v = 0$ and $v = 1$ states of the ${}^4\text{HeH}^+$ molecule. These new measurements also allowed for very precise determination of the low J rotation-vibration energy levels in the ground and $v = 1$ states, which will serve as new benchmarks for theorists to test *ab initio* calculations as higher level non-adiabatic, relativistic, and QED corrections are included. These measurements could also be used in a refinement of the empirical potential originally published by Coxon and Hajigeorgiou.²¹

ACKNOWLEDGMENTS

We would first like to acknowledge financial support from the National Science Foundation (CHE 12-13811). A.J.P., J.N.H., and C.R.M. are grateful to Mr. Paul A. Jenkins II for his assistance with setting up the spectrometer. J.N.H. is thankful for support from an NSF Graduate Research Fellowship (DGE 11-44245 FLLW). G.S.K. is thankful for financial support from a Gieseking scholarship. We would especially like to express gratitude to Professor Takeshi Oka for providing the glass discharge cell (Black Widow) along with the associated pumps and electronics.

- ¹S. Lepp, P. C. Stancil, and A. Dalgarno, *J. Phys. B* **35**, R57 (2002).
- ²S. Lepp, *Astrophys. Space Sci.* **285**, 737 (2003).
- ³T. R. Hogness and E. G. Lunn, *Phys. Rev.* **26**, 44 (1925).
- ⁴D. E. Tolliver, G. A. Kyrala, and W. H. Wing, *Phys. Rev. Lett.* **43**, 1719 (1979).
- ⁵P. Bernath and T. Amano, *Phys. Rev. Lett.* **48**, 20 (1982).
- ⁶A. Carrington, R. A. Kennedy, T. P. Softley, P. G. Fournier, and E. G. Richard, *Chem. Phys.* **81**, 251 (1983).
- ⁷C. E. Blom, K. Möller, and R. R. Filgueira, *Chem. Phys. Lett.* **140**, 489 (1987).
- ⁸Z. Liu and P. B. Davies, *J. Chem. Phys.* **107**, 337 (1997).
- ⁹M. W. Crofton, R. S. Altman, N. N. Haese, and T. Oka, *J. Chem. Phys.* **91**, 5882 (1989).
- ¹⁰D.-J. Liu, W.-C. Ho, and T. Oka, *J. Chem. Phys.* **87**, 2442 (1987).
- ¹¹F. Matsushima, T. Oka, and K. Takagi, *Phys. Rev. Lett.* **78**, 1664 (1997).
- ¹²Z. Liu and P. B. Davies, *Phys. Rev. Lett.* **79**, 2779 (1997).
- ¹³K. Pachucki and J. Komasa, *J. Chem. Phys.* **137**, 204314 (2012).
- ¹⁴J. Komasa, K. Piszczatowski, G. Łach, M. Przybytek, B. Jeziorski, and K. Pachucki, *J. Chem. Theory Comput.* **7**, 3105 (2011).
- ¹⁵R. E. Moss, *J. Phys. B* **32**, L89 (1999).
- ¹⁶L. Lodi, O. L. Polyansky, J. Tennyson, A. Aljiah, and N. F. Zobov, *Phys. Rev. A* **89**, 032505 (2014).
- ¹⁷W.-C. Tung, M. Pavanello, and L. Adamowicz, *J. Chem. Phys.* **137**, 164305 (2012).
- ¹⁸M. Stanke, D. Kędziera, M. Molski, S. Bubin, M. Barysz, and L. Adamowicz, *Phys. Rev. Lett.* **96**, 233002 (2006).
- ¹⁹S. Bubin, M. Stanke, D. Kędziera, and L. Adamowicz, *Phys. Rev. A* **76**, 022512 (2007).
- ²⁰M. Stanke, D. Kędziera, S. Bubin, and L. Adamowicz, *Phys. Rev. A* **77**, 022506 (2008).
- ²¹J. A. Coxon and P. G. Hajigeorgiou, *J. Mol. Spectrosc.* **193**, 306 (1999).

- ²²D. M. Bishop and L. M. Cheung, *J. Mol. Spectrosc.* **75**, 462 (1979).
- ²³J. N. Hodges, A. J. Perry, P. A. Jenkins, B. M. Siller, and B. J. McCall, *J. Chem. Phys.* **139**, 164201 (2013).
- ²⁴B. M. Siller, M. W. Porambo, A. A. Mills, and B. J. McCall, *Opt. Exp.* **19**, 24822 (2011).
- ²⁵K. N. Crabtree, J. N. Hodges, B. M. Siller, A. J. Perry, J. E. Kelly, P. A. Jenkins, and B. J. McCall, *Chem. Phys. Lett.* **551**, 1 (2012).
- ²⁶J. Ye, L.-S. Ma, and J. L. Hall, *J. Opt. Soc. Am. B* **15**, 6 (1998).
- ²⁷C. S. Gudeman, M. H. Begemann, J. Pfaff, and R. J. Saykally, *Phys. Rev. Lett.* **50**, 727 (1983).
- ²⁸L. S. Rothman, I. E. Gordon, Y. Babikov, A. Barbe, D. Chris Benner, P. F. Bernath, M. Birk, L. Bizzocchi, V. Boudon, L. R. Brown, A. Campargue, K. Chance, E. A. Cohen, L. H. Coudert, V. M. Devi, B. J. Drouin, A. Fayt, J.-M. Flaud, R. R. Gamache, J. J. Harrison, J.-M. Hartmann, C. Hill, J. T. Hodges, D. Jacquemart, A. Jolly, J. Lamouroux, R. J. Le Roy, G. Li, D. A. Long, O. M. Lyulin, C. J. Mackie, S. T. Massie, S. Mikhailenko, H. S. P. Müller, O. V. Naumenko, A. V. Nikitin, J. Orphal, V. Perevalov, A. Perrin, E. R. Polovtseva, C. Richard, M. A. H. Smith, E. Starikova, K. Sung, S. Tashkun, J. Tennyson, G. C. Toon, V. G. Tyuterev, and G. Wagner, *J. Quant. Spectrosc. Radiat. Transf.* **130**, 4 (2013).
- ²⁹J. Purder, S. Civiš, C. E. Blom, and M. C. van Hemert, *J. Mol. Spectrosc.* **153**, 701 (1992).
- ³⁰C. M. Western, PGOPHER, a Program for Simulating Rotational Structure, University of Bristol, <http://pgopher.chm.bris.ac.uk>.
- ³¹See supplementary material at <http://dx.doi.org/10.1063/1.4895505> for the fit details of each experimentally measured transition.



Contents lists available at ScienceDirect

Journal of Molecular Spectroscopy

journal homepage: www.elsevier.com/locate/jms

Note

High-precision *R*-branch transition frequencies in the ν_2 fundamental band of H_3^+ Adam J. Perry^a, James N. Hodges^a, Charles R. Markus^a, G. Stephen Kocheril^a, Benjamin J. McCall^{a,b,*}^a Department of Chemistry, University of Illinois, Urbana, IL 61801, USA^b Department of Astronomy, University of Illinois, Urbana, IL 61801, USA

ARTICLE INFO

Article history:

Received 10 July 2015

In revised form 4 September 2015

Available online xxxxx

Keywords:

Rovibrational spectroscopy
High-precision spectroscopy
Sub-Doppler spectroscopy
Ion spectroscopy
 H_3^+

ABSTRACT

The H_3^+ molecular ion has served as a long-standing benchmark for state-of-the-art *ab initio* calculations of molecular potentials and variational calculations of rovibrational energy levels. However, the accuracy of such calculations would not have been confirmed if not for the wealth of spectroscopic data that has been made available for this molecule. Recently, a new high-precision ion spectroscopy technique was demonstrated by Hodges et al., which led to the first highly accurate and precise (\sim MHz) H_3^+ transition frequencies. As an extension of this work, we present ten additional *R*-branch transitions measured to similar precision as a next step toward the ultimate goal of producing a comprehensive high-precision survey of this molecule, from which rovibrational energy levels can be calculated.

© 2015 Elsevier Inc. All rights reserved.

As the simplest polyatomic molecule, H_3^+ serves as an important benchmark system for *ab initio* calculation of molecular potential energy surfaces (PES) and spectra. The degree to which state-of-the-art calculations of the rovibrational transitions agree with experimental measurements is impressive, and is approaching the limit of the experimental uncertainty, typically on the order of 150–300 MHz (for a thorough review on previous laboratory spectroscopy of H_3^+ see Ref. [1]). Recent calculations [2] based on the highly accurate Born–Oppenheimer PES of Pavanello et al. [3], which included diagonal Born–Oppenheimer corrections (*i.e.* the adiabatic correction) and relativistic corrections, reproduce all known rovibrational energy levels for all isotopologues within 0.2 cm^{-1} . Shortly thereafter, Diniz et al. [4] developed a method for approximating the non-adiabatic effects using a “core-mass” approach whereby the nuclei are given coordinate-dependent masses as they undergo vibrational motion. Comparison to twelve high-precision (\sim 10 MHz) transitions arising from low-lying rovibrational energy levels yields an agreement between experiment and theory of $\sim 0.001 \text{ cm}^{-1}$ (\sim 30 MHz). Beyond these calculations Lodi and co-workers [5] have developed the first quantum electrodynamic correction surface for H_3^+ , which demonstrated the importance of including these effects, as well as the need for a more complete model for taking into account non-adiabatic effects.

Since the accuracy of theoretical calculations is now reaching the level of the experimental uncertainty, improved spectroscopic

measurements are needed in order to push the bounds of theoretical calculations. In this note we present ten new high-precision spectroscopic measurements in the ν_2 fundamental band of H_3^+ . These new frequencies, combined with those measured by Hodges et al. [6], represent a step towards completing a thorough high-precision spectroscopic survey for this important fundamental species. The spectra were acquired using the technique Noise-Immune Cavity Enhanced Optical Heterodyne Velocity Modulation Spectroscopy (NICE-OHVMS), in which traditional velocity modulation spectroscopy [7] is augmented with cavity enhancement and heterodyne modulation [8]. The instrument (described in detail in [6,9]) utilizes a high-power, continuous wave, optical parametric oscillator whose idler beam is coupled into an external optical cavity which surrounds a water-cooled AC positive column discharge of H_2 gas. Inside the cell, the pressure is maintained at 300–400 mTorr and the discharge is driven at frequencies of 40–50 kHz. Light transmitted through the cavity is detected by a fast photodiode detector whose signal is demodulated first at the heterodyne frequency (\sim 80 MHz) by a pair of electronic mixers and then again at twice the discharge frequency (80–100 kHz) by a pair of lock-in amplifiers. This detection scheme results in four channels of detection, producing signals from each heterodyne mixer that are in-phase and 90° out of phase (in quadrature) with the sinusoidal driving voltage of the discharge. Frequency calibration of the spectra is accomplished by measuring the difference in frequency between the pump and signal waves. Measurements of these beams are obtained with a near-infrared wavelength meter and optical frequency comb.

* Corresponding author at: Department of Chemistry, University of Illinois, Urbana, IL 61801, USA.

Due to the bi-directional nature and optical power enhancement of the external optical cavity, it is possible to perform sub-Doppler spectroscopy which enables high-precision line center measurements. Such a spectrum is illustrated in Fig. 1. Line centers are extracted via a simultaneous fit of all four detection channels to the sub-Doppler features. In the fit the line center, heterodyne detection angle, and full-width of the feature are all shared parameters between the four channels. Previous high-precision measurements were limited to transitions from lower- J levels and these new measurements have expanded the range up to $J = 6$. All newly measured transition frequencies are reported in Table 1. Uncertainties in the line centers are assigned as the standard deviation of a data set composed of at least five scans for each transition, and as a result are highly dependent on the signal-to-noise ratio of the sub-Doppler features. The precision to which these lines have been measured represents an improvement over previous measurements of two orders of magnitude for most of the transitions. It is worth noting that the works of Oka [10], and Lindsay et al. [1] appear to be highly accurate, and their claimed uncertainties may be a bit conservative.

The only new measurement that falls outside of the stated uncertainties of the previous work is that of $R(3,3)^u$, for which we record a frequency that is 15 MHz lower than that reported by Wu et al. [11]. Though this discrepancy is not completely unreasonable (1.5σ), we set out to confirm this frequency by performing a second, independent measurement of this transition. Doing so yielded the same value (to within our specified uncertainty). To eliminate any possibility of an unexpected systematic error in our frequency calibration, we immediately remeasured the $R(1,0)$ transition, which was in good agreement with Hodges et al. and Wu et al., and we still obtain the same value for its line center. These tests leave us confident in the accuracy of our $R(3,3)^u$ measurement.

Table 1

Newly measured rovibrational transitions in the ν_2 fundamental band of H_3^+ and a comparison to previous values. All units are in MHz.

Transition ^a	This work	Previous	Diff.
$R(4,3)^l$	86778433.66(76)	86778225(300) ^b	208.66
$R(3,3)^u$	87480191.43(117)	87480207(10) ^c	-15.57
$R(3,2)^u$	87640201.59(254)	87640158(300) ^b	43.59
$R(3,1)^u$	87789812.71(130)	87789754(300) ^b	58.71
$R(3,0)$	87844195.67(122)	87844077(300) ^b	118.67
$R(5,5)^l$	88620962.34(144)	88620809(300) ^b	153.34
$R(6,6)^l$	90368280.18(102)	90368359(150) ^d	-78.82
$R(4,3)^u$	90394720.09(232)	90394651(150) ^d	69.09
$R(4,2)^u$	90673895.29(179)	90673968(300) ^d	-72.71
$R(4,1)^u$	90831978.56(177)	90832078(150) ^d	-99.44

^a Labels for these transitions refer to (J, G) ; for more details on H_3^+ notation see [1].

^b Ref. [10].

^c Ref. [11].

^d Ref. [12].

Work is now underway to extend the frequency coverage of the spectrometer which will allow us to measure P and Q branch transitions in this band. Once this is accomplished it will be possible to begin measuring energy level spacings in the ground vibrational state with precision that has never before been achieved. Upon completion of the fundamental band measurements, a survey of transitions in the $2\nu_2^{\ell=2} \leftarrow \nu_2$ hot band along with transitions in the first overtone band ($2\nu_2^{\ell=2} \leftarrow 0$) will allow us to determine relative energy spacings among levels within the *ortho* and *para* species. Finally, a fit of the ground state energy levels to a modified Watson-type Hamiltonian will allow for absolute energy levels to be extracted. Once completed this work will equip theorists with a complete and highly precise list of experimentally determined

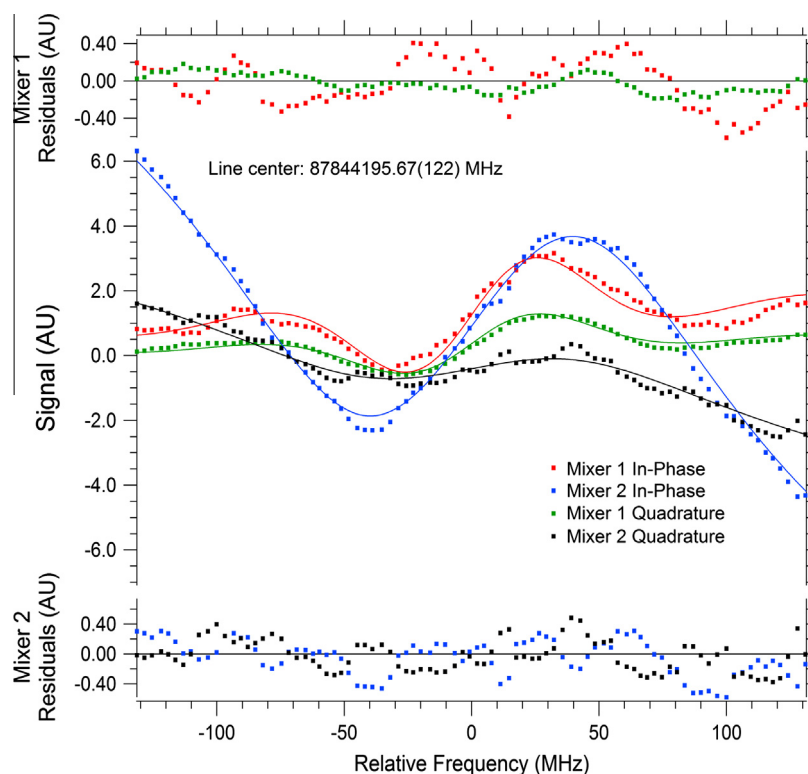


Fig. 1. A NICE-OHVMS scan of sub-Doppler feature of the $R(3,0)$ fundamental band transition of H_3^+ centered at 87844195.67(122) MHz. Signals from each of the four detection channels are shown (dots) and are fitted simultaneously (solid traces) with the line center as a shared parameter. The odd symmetry of the line shapes is a result of the applied modulation scheme.

rovibrational energy levels for this critically important molecular system.

Acknowledgments

This work was funded by the National Science Foundation (PHY 14-04330). J.N.H. is grateful for support from an NSF Graduate Research Fellowship (DGE 11-44245 FLLW). G.S.K. is thankful for financial support from a Giesecking scholarship.

References

- [1] C. Lindsay, B.J. McCall, *J. Mol. Spectrosc.* 210 (2001) 60–83.
- [2] O.L. Polyansky, A. Aljiah, N.F. Zobov, I.I. Mizus, R.I. Ovsyannikov, J. Tennyson, L. Lodi, T. Szidarovszky, A.G. Császár, *Philos. Trans. A Math. Phys. Eng. Sci.* 370 (2012) 5014–5027.
- [3] M. Pavanello, L. Adamowicz, A. Aljiah, N.F. Zobov, I.I. Mizus, O.L. Polyansky, J. Tennyson, T. Szidarovszky, A.G. Császár, *J. Chem. Phys.* 136 (2012) 184303.
- [4] L.G. Diniz, J.R. Mohallem, A. Aljiah, M. Pavanello, L. Adamowicz, O.L. Polyansky, J. Tennyson, *Phys. Rev. A* 88 (2013) 032506.
- [5] L. Lodi, O.L. Polyansky, J. Tennyson, A. Aljiah, N.F. Zobov, *Phys. Rev. A* 89 (2014) 032505.
- [6] J.N. Hodges, A.J. Perry, P.A. Jenkins II, B.M. Siller, B.J. McCall, *J. Chem. Phys.* 139 (2013) 164201.
- [7] C. Gudeman, M. Begemann, J. Pfaff, R. Saykally, *Phys. Rev. Lett.* 50 (1983) 727–731.
- [8] B.M. Siller, M.W. Porambo, A.A. Mills, B.J. McCall, *Opt. Express* 19 (2011) 24822–24827.
- [9] K.N. Crabtree, J.N. Hodges, B.M. Siller, A.J. Perry, J.E. Kelly, P.A. Jenkins II, B.J. McCall, *Chem. Phys. Lett.* 551 (2012) 1–6.
- [10] T. Oka, *Philos. Trans. R. Soc. A* 303 (1981) 543–549.
- [11] K.-Y. Wu, Y.-H. Lien, C.-C. Liao, Y.-R. Lin, J.-T. Shy, *Phys. Rev. A* 88 (2013) 032507.
- [12] C. Lindsay, R.M. Rade, T. Oka, *J. Mol. Spectrosc.* 210 (2001) 51–59.